Mechanisms of Fibroblast Growth Factor 2 Intracellular Processing: A Kinetic Analysis of the Role of Heparan Sulfate Proteoglycans†

Gizette V. Sperinde and Matthew A. Nugent*

Departments of Biochemistry and Ophthalmology, Boston University School of Medicine, Boston, Massachusetts 02118

Received September 27, 1999; Revised Manuscript Received January 5, 2000

ABSTRACT: The interaction of fibroblast growth factor 2 (FGF-2) with heparan sulfate proteoglycans (HSPG) has been demonstrated to enhance receptor binding and alter the intracellular distribution of internalized FGF-2. In the present study, the intracellular fate of FGF-2 was analyzed in vascular smooth muscle cells (VSMC) under native and HSPG-deficient conditions. HSPG-deficient cells were generated by treatment with sodium chlorate. Cells were incubated with FGF-2 at 37 °C for prolonged periods (0−48 h) to allow for FGF-2 uptake and processing. Processing of FGF-2 occurred in stages. Initially a family of low molecular weight (LMW) fragments (4−10 kDa) were detected that accumulated to much higher (∼10-fold) levels in native compared to heparan sulfate-deficient cells. Pulse−chase experiments revealed that the half-life of these LMW intermediates was significantly greater in native (∼18 h) compared to HSPG-deficient cells (∼4 h). Rate constants for FGF-2 processing were derived by modeling the uptake and processing of FGF-2 as a set of first-order differential equations. The kinetic analysis indicated that the greatest differences between native and HSPG-deficient VSMC was in the formation of LMW and further suggested that these FGF-2 products appear to represent a stable subpool of internal FGF-2 that is favored in cells that contain HSPG. Thus, HSPG might function as a cellular switch between immediate and prolonged signal activation by heparin-binding growth factors such as FGF-2. In the absence of HSPG, FGF-2 can interact with and activate its receptor, yet in the presence of HSPG, FGF-2 might be able to mediate prolonged or unique biological responses through intracellular processes.

Fibroblast growth factor 2 (FGF-2)[1] belongs to a family of at least 18 related polypeptides (*1*). At the cell surface, FGF-2 binds to tyrosine kinase receptors (FGFR1−4) as well as heparan sulfate proteoglycans (HSPG) (*2*−*4*). The biological role of the FGFRs has been characterized extensively (*3*). The interaction of FGF-2 with FGFR has been shown to result in the activation of several intracellular signaling cascades, which include activation of the mitogen-activated protein kinases and phospholipase Cγ, leading to cell proliferation, migration, and differentiation (*1*, *3*). FGF-2 binding to HSPG has been shown to modulate FGF-2 activity at a number of levels. It has been shown that the interaction of FGF-2 with HSPG increases the binding affinity of FGF-2 for FGFR, leading to increased cellular response (*5*−*9*). Recent evidence suggests a direct involvement of HSPG in signaling, such as the FGF-2-mediated dephosphorylation of syndecan 4 (*10*).

There have been numerous reports implicating the involvement of internalized FGF-2 or its receptors in mediating intracellular biological function (*7*, *11*). Upon binding, FGF-2/FGFR complexes are internalized. The complexes are subsequently directed to endosomes and lysosomes, where degradation of ligand, receptor, or the entire complex occurs (*12*, *13*). Several studies have demonstrated that this process is inhibited by the addition of lysosomal inhibitors in various cell types, including venular endothelial cells (*14*), chinese hamster lung fibroblasts (*15*), and bovine aortic endothelial cells (*16*). However, there have been indications that FGF-2, its receptors, and HSPG may also be directed to other intracellular destinations (*17*−*20*). Indeed, there have been reports of nuclear localization of FGF-2 in a variety of cell types (*11*, *14*, *21*). Nuclear accumulation of FGF-2 has been shown to be cell-cycle-dependent, occurring in the G1−S transition (*16*). FGFR have also been shown to be localized to the nucleus and perinuclear region, where it is suggested that they might continue to signal (*20*, *22*, *23*). The role of HSPG in modulating the intracellular fate of FGF-2 and its receptors is poorly understood. HSPG are constitutively internalized and degraded, through both lysosomal as well as nonlysosomal pathways in rat ovarian granulosa cells (*24*). Heparan sulfate has also been found localized in the nuclei of hepatocytes (*21*, *25*, *26*). We have recently shown that HSPG inhibit the accumulation of FGF-2 degradation products in the medium of vascular smooth muscle cells (VSMC) (*11*).

† This work was supported in part by Grants R01HL56200 and P01HL46902 from the National Institutes of Health and by Departmental grants from the Massachusetts Lions Eye Research Fund and Research to Prevent Blindness, Inc.

* Correspondence should be addressed to this author at the Department of Biochemistry, Room K225, Boston University School of Medicine, 716 Albany St., Boston, MA 02118. Fax 617 638-5339; E-mail nugent@biochem.bumc.bu.edu.

[1] Abbreviations: BSA, bovine serum albumin; DMEM, Dulbecco's modified Eagle's medium; FGF-2, fibroblast growth factor 2; FGFR, fibroblast growth factor receptor; HSPG, heparan sulfate proteoglycans; LMW, low molecular weight; MAPK, mitogen-activated protein kinases; NGF, nerve growth factor; TCA, trichloroacetic acid; VSMC, vascular smooth muscle cells.

10.1021/bi992243d CCC: $19.00
Published on Web 03/10/2000

In the present study, the role of HSPG in modulating the intracellular degradation of FGF-2 was investigated in VSMC. VSMC were chosen for these studies for their sensitive regulation by FGF-2, heparin, and HSPG in vivo and in vitro (*27*−*32*). VSMC were rendered HSPG-deficient by treatment with sodium chlorate. The consequences of the presence and absence of HSPG on the intracellular degradation of FGF-2 was analyzed. The intracellular processing of FGF-2 occurred in stages. First, low molecular weight (LMW) fragments (4−10 kDa) were detected in both native and HSPG-deficient VSMC. However, the LMW fragments accumulated to much higher levels in native cells as compared with HSPG-deficient VSMC. LMW fragments of FGF-2 constituted the greatest fraction of internalized growth factor in native VSMC. Pulse−chase experiments showed a product/precursor relationship between 18 kDa FGF-2 and the low molecular weight (LMW) intermediates. The half-life of these LMW intermediates was significantly greater in native VSMC (8−18 h) as compared with HSPG-deficient VSMC (2−4 h). Inhibition of lysosomal degradation by chloroquine treatment greatly reduced the intracellular concentrations of FGF-2 in native VSMC but had no effect on HSPG-deficient VSMC. There are distinct differences in FGF-2 processing in the presence and absence of HSPG in VSMC. It is possible that the regulated processing of FGF-2 by HSPG has important biological consequences.

MATERIALS AND METHODS

Materials. Human recombinant FGF-2 was from Scios-Nova, Inc. (Mountain View, CA).

^{125}I-FGF-2 was prepared by a modification of the Bolton−Hunter procedure (*6*). This method has been demonstrated to produce active ^{125}I-FGF-2 as determined by its ability to stimulate DNA synthesis in quiescent Balb/c3T3 cells. The specific activity ranged from 80 to 90 μCi/μg. [^{35}S]Sulfate and ^{125}I-Bolton−Hunter reagent were from DuPont NEN (Boston, MA). Sodium chlorate ($NaClO_3$) was obtained from Fluka (Ronkonkoma, NY). *p*-Nitrophenyl phosphate (PNP), Nonidet P-40, and other reagent-grade chemicals were from Sigma (St. Louis, MO).

Cell Culture. Vascular smooth muscle cells (VSMC) were used between passages 4 and 8. VSMC, isolated as described (*33*), were from Coriell Cell Repositories (Camden, NJ). Cells were maintained in 75 cm^2 vented culture flasks (Costar, Cambridge, MA) in Dulbecco's modified Eagle's medium (DMEM, low glucose, Life Technologies, Inc.), supplemented with 20% fetal bovine serum (FBS) (Life Technologies, Inc.), penicillin (100 units/mL), streptomycin (100 μg/mL), and glutamine (2 mM). Cell number was determined with a Coulter counter, or relative cell numbers were determined by acid phosphatase quantitation (*34*). Briefly, cells were incubated in 0.1M sodium acetate (pH 5.5), 0.1% Triton X-100, and 10 mM *p*-nitrophenyl phosphate (Sigma 104 phosphatase substrate) for 45 min at 37 °C. The reaction was stopped by the addition of 1 N NaOH and absorbance was determined at 410 nm with a Shimadzu UV−vis spectrophotometer**.**

Chlorate Treatment. Chlorate treatment was performed as described previously (*11*) to generate HSPG-deficient VSMC. To obtain similar cell numbers for native and chlorate-treated VSMC at the end of the chlorate treatment procedure, chlorate-treated cells were plated at a higher initial seeding density. VSMC were plated at 25 000/cm^2 for native and at 37 500/cm^2 for chlorate-treated cells in low-glucose DMEM, 0.5% dialyzed calf serum (DCS) (Sigma), and glutamine (2 mM). Following cell attachment, approximately (∼4 h), cells were treated with or without sodium chlorate (75 mM final concentration) for 48 h at 37 °C.

Cellular Fractionation. Cell fractionation was performed as described previously (*11*). Briefly, cells were washed three times with ice-cold binding buffer (DMEM, 25 mM HEPES, and 0.05% gelatin) and cell-surface-bound ^{125}I-FGF-2 was removed by sequential extraction with a high-salt buffer [20 mM HEPES and 1 M NaCl, pH 7.4; 0.5 mL/well for 5 s; followed by a wash with phosphate-buffered saline (PBS)] and high salt/acid buffer (10 mM sodium acetate and 1 M NaCl, pH 5, for 5 min; followed by a wash with PBS). Cells were trypsinized with 0.5 mL of 0.01% trypsin and 0.53 mM EDTA (Life Technologies, Inc.) per well. Trypsinization was stopped by the addition of 50 μL/well calf serum (Hyclone, UT). Cell suspensions were centrifuged for 30 s at 10000*g*. Cell pellets were resuspended by briefly vortexing in 200 μL of homogenization buffer (10 mM HEPES, pH 7.9, 10 mM KCl, 0.1 mM EDTA, 0.1 mM EGTA, 1 mM DTT, and 0.5 mM PMSF) and incubated on ice for 15 min (*20*). After this incubation, 12.5 μL of a 10% Nonidet P-40 solution was added to each tube and the samples were vortexed vigorously for 10 s. This was followed by another centrifugation, 30 s at 10000*g*. The supernatant was collected as the cytoplasmic fraction. The crude nuclear pellet was washed two additional times by repeating the procedure outlined above. The nuclear pellet was then resuspended in 100 μL of homogenization buffer. Radioactivity in these fractions was quantitated by counting in a Packard Model 5650 γ counter. Boiling Laemmli sample buffer was added to the fractions obtained for electrophoretic analysis. Virtually full recovery of the cytoplasmic fraction was observed, based on acid phosphatase quantitation in the cytoplasmic fraction as compared with nonfractionated, whole cells. Based on recovery and quantitation of the lysosomal contaminant, acid phosphatase, in the nuclear fraction (*34*), less than 0.5% lysosomal contamination was found in the nuclear fraction (*11*).

TCA Precipitation. Samples were subjected to TCA precipitation to separate incorporated radioactivity from unincorporated or small fragments. Briefly, 5 μL of sample was combined with 5 μL of BSA solution (10 mg/mL), 10 μL of KI (10 mM), and 70 μL of NaCl (150 mM). Then 12.5 μL of 100% TCA (ice cold) was added to the final mixture to precipitate proteins. The precipitate was collected by centrifugation at 10000*g* for 10 min. Radioactivity in the supernatant and pellet was quantitated with a γ counter.

Gel Electrophoresis. Cell layers were solubilized in boiling Laemmli sample buffer. Samples were normalized to relative cell numbers on the basis of acid phosphatase quantitation and subjected to SDS−polyacrylamide gel electrophoresis (PAGE) (16% running gel, 5% stacking gel) (*11*). Bio-Rad prestained standards were used for molecular mass calibration. ^{125}I-labeled protein bands were visualized through exposure of the gel onto a phosphorimager SF phosphor plate (Molecular Dynamics).

Rate Constants. Numerical analysis was based on first-order reactions. Each step in the FGF-2 binding, internalization, and processing pathway was represented as a chemical reaction, where product formation was dependent on the first-order concentration of the precursor pool. All models were fitted to experimental data and assumed uniform binding sites for FGF-2 on the cell surface, for both the high- and low-affinity receptors. Cooperative and competitive interactions were assumed to be negligible. Nonspecific interactions were low and assumed to be negligible at the concentration ranges of the experiments (*11*). In each case, a series of equations were derived as a model to describe the specific experiment and these were solved simultaneously and compared with experimental data, to yield kinetic rate constants. The terms are as follows: [F] is the concentration of soluble FGF-2 in the medium at any time, [R] is the concentration of free FGFR remaining at any time, [F·R] is the concentration of FGF-2/FGFR complexes at any time, [H] is the concentration of free HSPG sites present at any time, [F·H] is the concentration of FGF-2/HSPG complexes, [Fe] is the concentration of internalized FGF-2 (18 and 16 kDa), [F(LMW)] is the concentration of processed low molecular fragments of FGF-2, [F(deg)] is the concentration of TCA-soluble byproducts of FGF-2 secreted into the medium, k_{onR} is the rate constant for the forward reaction of FGF-2 binding to FGFR, k_{offR} is the rate constant for the dissociation of the FGF-2/FGFR complex, k_{onH} is the rate constant for the forward reaction of FGF-2 binding to HSPG, k_{offH} is the rate constant for the dissociation of the FGF-2/HSPG complex, k_{eR} is the rate constant for the internalization of FGF-2/FGFR complex, k_{eH} is the rate constant for the internalization of FGF-2/HSPG complex, k_{deg} is the rate constant for the degradation of FGF-2 into TCA-soluble fragments detected in the medium, and k_{LMW} is the rate constant for the processing of internalized FGF-2 into low molecular weight fragments.

Endocytic Reactions. Endocytosis was simulated on the basis of reactions 1−4. At relatively short time scales, the assumption that internalized FGF-2 is virtually completely in the form of high molecular weight FGF-2 still holds. It was assumed that HSPG and receptors internalize FGF-2 independently. Downstream reactions were accounted for by the inclusion of k_d, which represents the sum of the rate constants of the subsequent reactions.

$$\text{Reaction 1} \qquad [F] + [R] \underset{k_{offR}}{\overset{k_{onR}}{\rightleftarrows}} [F\cdot R]$$

$$\text{Reaction 2} \qquad [F] + [H] \underset{k_{offH}}{\overset{k_{onH}}{\rightleftarrows}} [F\cdot H]$$

$$\text{Reaction 3} \qquad [F\cdot R] \xrightarrow{k_{eR}} [Fe]$$

$$\text{Reaction 4} \qquad [F\cdot H] \xrightarrow{k_{eH}} [Fe]$$

The above reactions were described by a series of first-order differential equations, shown below:

$$\frac{d[F\cdot R]}{dt} = k_{onR}[F][R] - k_{offR}[F\cdot R] - k_{eR}[F\cdot R] \quad (1)$$

$$\frac{d[F\cdot H]}{dt} = k_{onH}[F][H] - k_{offH}[F\cdot H] - k_{eH}[F\cdot H] \quad (2)$$

$$\frac{d[Fe]}{dt} = k_{eR}[F\cdot R] + k_{eH}[F\cdot H] - k_{deg}[Fe] \quad (3)$$

$$\frac{d[F]}{dt} = -\frac{d[F\cdot R]}{dt} - \frac{d[F\cdot H]}{dt} \quad (4)$$

To determine postinternalization events, all upstream reactions were evaluated simultaneously. Reactions 5 and 6 were included with reactions 1−4 to simulate the binding, internalization, and processing of FGF-2:

$$\text{Reaction 5} \qquad [Fe] \xrightarrow{k_{LMW}} [F(LMW)]$$

$$\text{Reaction 6} \qquad [Fe] \xrightarrow{k_{deg}} [F(deg)]$$

The above reactions were described by eqs 1 and 2 and the following processing reactions:

$$\frac{d[Fe]}{dt} = k_{eR}[F\cdot R] + k_{eH}[F\cdot H] - k_{LMW}[Fe] - k_{deg}[Fe] \quad (5)$$

$$\frac{d[F(LMW)]}{dt} = k_{LMW}[Fe] \quad (6)$$

$$\frac{d[F\ deg]}{dt} = k_{deg}[Fe] \quad (7)$$

$$\frac{d[F]}{dt} = -\frac{d[F\cdot R]}{dt} - \frac{d[F\cdot H]}{dt} - \frac{d[Fe]}{dt} - \frac{d[F(LMW)]}{dt} - \frac{d[F(deg)]}{dt} \quad (8)$$

An iterative process was used, in a computer simulation using FORTRAN on a 100 MHz Think Pad 560 (IBM), which numerically integrated the model equations, given a set of initial reaction rate constants, by a fourth-order Runge-Kutta step method. The values derived through the numerical integrator were then compared to experimental data and the difference (χ^2) was minimized with every iteration. The iterative procedure continued until theoretical values were obtained that minimize χ^2. This was done by reguessing for the values of the rate constants through the Levenberg−Marquardt method (*35*) and reintegrating the equations. The iteration stopped when the value of χ^2 was within 0.1% of the previous value.

RESULTS

LMW Fragments of FGF-2 Accumulate in Native VSMC. Endocytosis of a growth factor/receptor complex generally leads to the degradation of the complex. Degradation of either ligand or receptor has been regarded as a shut-off mechanism of the signaling process. However, FGF-2 has a relatively long intracellular half-life (*36*) as compared with non-heparin-binding mitogens (*37*), suggesting that intracellular degradation of FGF-2 is subject to regulation. Therefore, the role of HSPG in modulating FGF-2 catabolism was investigated. Secreted, processed byproducts of FGF-2 degradation had previously been shown to accumulate in the medium

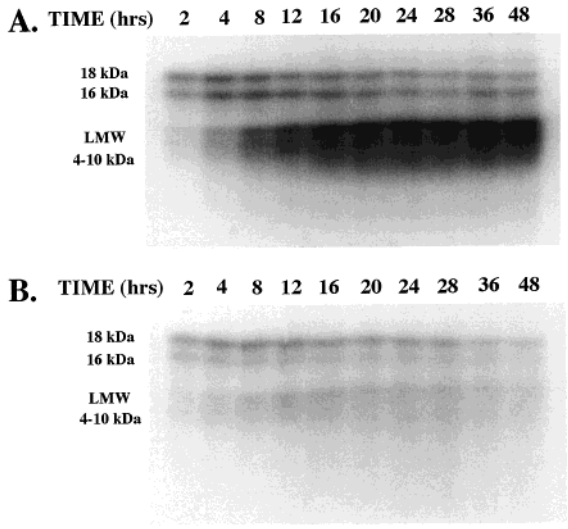

FIGURE 1: Intracellular processing of FGF-2 within native and HSPG-deficient VSMC. Native (A) and HSPG-deficient VSMC (B) were treated with ^{125}I-FGF-2 (0.28 nM) for the indicated times at 37 °C. At each time point, cell-surface-bound FGF-2 was removed, and cells were solubilized with boiling Laemmli sample buffer and applied to an SDS−16% polyacrylamide gel. Bands were visualized by the phosphorimager and quantitated with Image Quant software. Similar results were observed in four separate experiments.

with slower kinetics in native VSMC as compared with HSPG-deficient cells (*11*), suggesting that HSPG inhibit intracellular degradation of FGF-2.

The intracellular state of FGF-2 was analyzed at different stages of processing in native and HSPG-deficient VSMC. Cells were exposed to ^{125}I-FGF-2 at 37 °C to allow for uptake and processing. At each time point, cell-surface-associated ^{125}I-FGF-2 was removed (high ionic strength, low pH wash) and the cells were solubilized and subjected to SDS−PAGE analysis. At the earliest time points, the majority of the ^{125}I-FGF-2 was composed of 18 and 16 kDa forms. With increasing incubation times a group of LMW fragments of FGF-2 formed in both native and HSPG-deficient VSMC (Figure 1). Only native VSMC retained and accumulated significant amounts of the LMW fragments, suggesting that HSPG-deficient cells were able to process FGF-2 in a similar manner but were unable to retain the processed fragments. The relative intensities of the bands in each lane in Figure 1 were quantitated and the LMW fragments constituted the majority of the FGF-2 present in the native cells: greater than 70% after 16 h and 90% after 24 h (Figure 2). Within HSPG-deficient VSMC, the LMW fragments constituted a maximum of 30% of total intracellular FGF-2 present after prolonged incubations (24−36 h). These data suggest that the large differences in the total intracellular levels of FGF-2 in native versus HSPG-deficient VSMC arose largely from the increased accumulation of LMW fragments within native cells. The intracellular levels of the 18 and 16 kDa species of FGF-2 in the HSPG-deficient VSMC were virtually the same as in the native cells. However, LMW fragments reached a rapid steady state, followed by a steady decline at approximately 12 h in HSPG-deficient cells. At the later time points, native cells retained 10-fold higher concentrations of LMW fragments, as compared to HSPG-deficient VSMC.

LMW Fragments Are Cleared at a Slower Rate in Native VSMC. Pulse chase experiments were performed to isolate the relevant FGF-2 intracellular processing steps that resulted

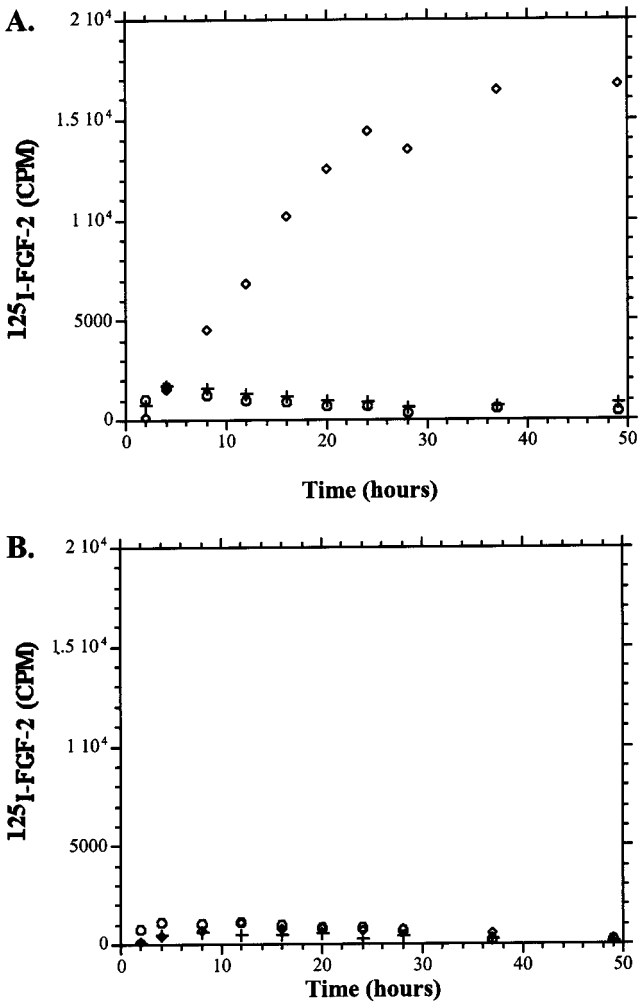

FIGURE 2: Total composition of 18 kDa, 16 kDa, and LMW fragments within native and HSPG-deficient VSMC. ^{125}I-FGF-2 was added to native (A) and HSPG-deficient (B) VSMC (0.28 nM) for the indicated times at 37 °C. At each time point, cell-surface-bound FGF-2 was removed, and cells were solubilized in boiling Laemmli sample buffer and applied to an SDS−polyacrylamide gel (Figure 1). Percentage radioactivity in each band from Figure 1 was determined by a phosphorimager. ^{125}I radioactivity was calculated in bands corresponding to 18 (+), 16 (○), and LMW (◇) fragments by multiplying the relative composition of each lane by the total amount of radioactivity per lane, as determined by γ counting. The results presented are representative of the average of triplicate determinations. Similar results were observed in three separate experiments.

in the observed differences in uptake of FGF-2 in native and HSPG-deficient VSMC. Native and HSPG-deficient VSMC were exposed to ^{125}I-FGF-2 for 2 h at 37 °C (pulse). After this pulse period, medium containing ^{125}I-FGF-2 and cell-surface-bound ^{125}I-FGF-2 were removed. Fresh medium was added back to the cells and the incubation continued for various times at 37 °C for the chase. At each time point, medium was collected and the cells were extracted for analysis of processed FGF-2. LMW fragments were the primary constituent, after approximately 12 h of chase period (Figure 3). After a 2 h exposure to FGF-2, both native and HSPG-deficient VSMC accumulated similar levels of LMW fragments, which allowed for a direct comparison of FGF-2 clearance under these conditions. Comparison of internal FGF-2 immediately after the pulse period to that after 2 h of chase (t = 0 and 2 h in Figure 3) suggests that the

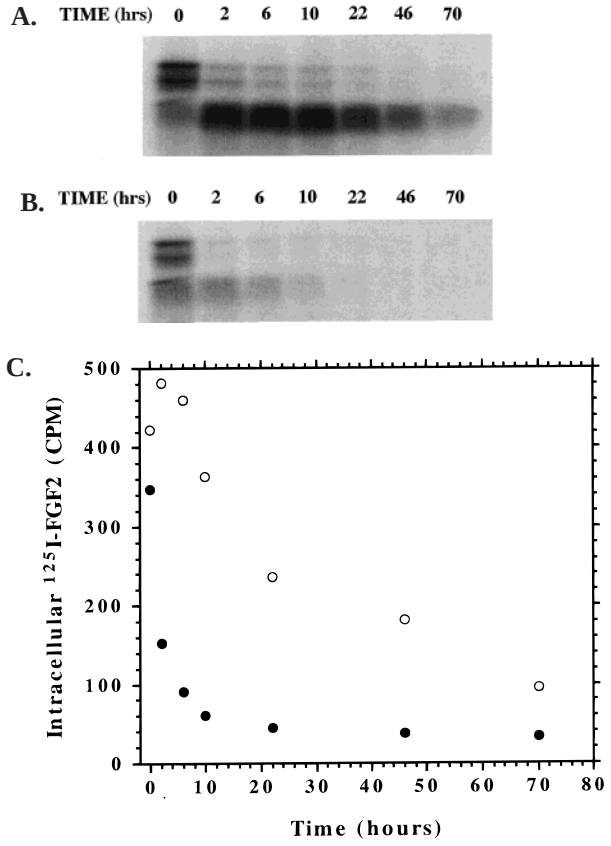

FIGURE 3: Intracellular clearance of processed FGF-2 in native and HSPG-deficient VSMC. Native (A) and HSPG-deficient VSMC (B) were treated with ^{125}I-FGF-2 (0.28 nM) for 2 h at 37 °C (pulse), to allow for ^{125}I-FGF-2 internalization. After this time, cells were washed with binding buffer and high-salt, low-pH buffer (see Materials and Methods) to remove all soluble and cell-bound ^{125}I-FGF-2. Medium was added back to the cells together with unlabeled FGF-2 at a final concentration of 0.28 nM (chase, time = 0 h). Cells were incubated for the indicated times at 37 °C. Cell layers were solubilized with boiling Laemmli sample buffer, radioactivity was quantitated by γ counting (C) in both native (○) and HSPG-deficient VSMC (●) and samples were applied to SDS−PAGE. The results presented represent the pooled fractions of triplicate determinations.

formation of LMW fragments occurred rapidly. Additionally, a product/precursor relationship existed between the higher molecular weight forms of initially internalized, 18 kDa FGF-2 and the processed fragments that were generated during prolonged exposures. Total radioactivity in each lane was quantitated (Figure 3C). The half-life of the LMW intermediates was greatly prolonged in native VSMC (~18 h; apparent first-order rate constant of 0.04 h^{-1}) as compared with HSPG-deficient VSMC (~4 h; apparent first-order rate constant of 0.17 h^{-1}).

The clearance of FGF-2 comprises a sum of processes that lead to the eventual excretion of small molecular weight FGF-2 degradation products. Although TCA soluble processed fragments of FGF-2 comprised the majority of the cellular excreted FGF-2, experiments were conducted to evaluate the extent of FGF-2 recycling. When VSMC were allowed to excrete ^{125}I-FGF-2 under conditions where a large excess of unlabeled FGF-2 was included in the medium to prevent rebinding of recycled intact ^{125}I-FGF-2, no significant intact ^{125}I-FGF-2 was detected in the incubation medium (data not shown). Therefore, it is unlikely that recycling of FGF-2 occurs to any significant degree in VSMC under these experimental conditions.

Table 1: Kinetic Constants for FGF-2 Internalization in Native VSMC[a]

kinetic constants	native VSMC	HSPG-deficient VSMC
k_{eR} (h^{-1})	0.72	2.16
k_{eH} (h^{-1})	0.29	N/A

[a] Data for the amounts of FGF-2 in the medium, bound to HSPG, bound to receptor sites, and inside the cell were collected over a 30-min time course and were simultaneously fit to eqs 1−4. The computer simulation minimized the difference between the model and the data. Endocytosis rate constants for receptors, k_{eR}, and HSPG, k_{eH}, were determined.

LMW Are Generated with Rapid Kinetics in Native VSMC. The differences in FGF-2 processing between native and HSPG-deficient VSMC may arise at various stages of growth factor binding, endocytosis, intracellular processing, and excretion. It has been shown that the presence of HSPG alters FGF-2 binding to cell surface receptors (*6*, *8*, *9*). To identify the steps in the FGF-2 processing pathway that are controlled by HSPG, a kinetic analysis of FGF-2 endocytosis, intracellular processing, and excretion was performed.

To isolate the endocytic rate constant for FGF-2 at 37 °C, short time scale internalization of FGF-2 was carried out to avoid the complexities of downstream processing events. Cells were exposed to ^{125}I-FGF-2 over a 30 min time course and the amount of ^{125}I-FGF-2 in each experimental compartment (medium, cell surface, and intracellular) was measured. At each time point, the medium was collected and ^{125}I-FGF-2 content was determined by TCA precipitation. HSPG and receptor-bound FGF-2 were removed and counted through high-salt and low-pH extractions sequentially. Internalized FGF-2 was extraction with 0.5% Triton X-100 in PBS. The endocytic rate constants were determined by fitting eqs 1−4 to the experimental data (see Materials and Methods) (Table 1). The apparent receptor endocytic rate constant was 3-fold greater for HSPG-deficient VSMC as compared with native cells. This may reflect a higher percentage of FGF-2 internalization through receptors in HSPG-deficient VSMC.

To identify the relative extent to which slow production or fast excretion of LMW fragments lead to the differences observed in the levels of these fragments formed in native and HSPG-deficient cells (Figure 1, panels A and B, respectively), a kinetic analysis was performed in conjunction with process simulation based on reactions 1−6 and eqs 1−8 (Figures 4 and 5). Cells were exposed to ^{125}I-FGF-2 at 37 °C to allow for uptake and processing. At each time point, cell-surface-associated ^{125}I-FGF-2 was removed (high ionic strength, low pH wash) and the cells were solubilized and subjected to SDS−PAGE analysis. Processed ^{125}I-FGF-2 fragments excreted into the medium were quantitated by TCA precipitation. Internalized FGF-2, visualized on gels as 18 and 16 kDa bands, were grouped as one pool. The results of the process simulation best fit are shown in Figures 4 and 5. The rate constant for LMW fragment formation was increased by greater than 6-fold within native as compared with HSPG-deficient VSMC, suggesting that native cells produce LMW fragments at faster rates (Table 2). The rate constant governing the overall excretion of degraded FGF-2 into the medium was similar within both native and HSPG-deficient cells. This excretion rate did not reflect the much

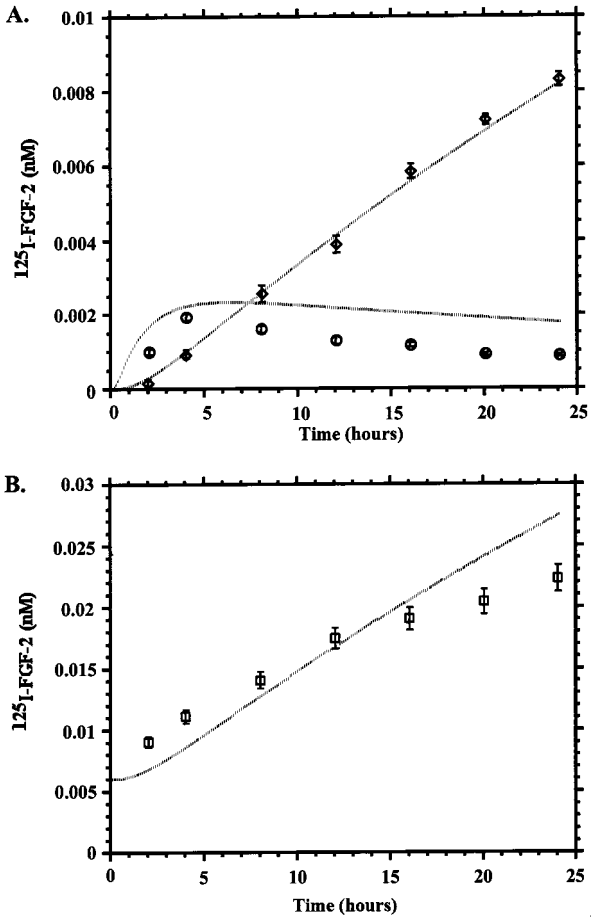

FIGURE 4: FGF-2 processing and secretion within native VSMC. ^{125}I-FGF-2 was added to native VSMC (0.28 nM) for the indicated times at 37 °C. At each time point, cell-surface-bound FGF-2 was removed, medium was subject to TCA precipitation, and cells were solubilized in boiling Laemmli sample buffer and applied to an SDS−polyacrylamide gel. Radioactivity in each lane was quantitated with a phosphorimager. ^{125}I radioactivity was calculated in bands corresponding to 18 + 16 kDa (○) and LMW (◇) (A), and TCA-soluble (degraded FGF-2) radioactivity was measured in the medium (B) (□). The results represent the averages of triplicate determinations. First-order differential equations (eqs 1−8) were fit to the data to produce the theoretical isotherms (lines shown).

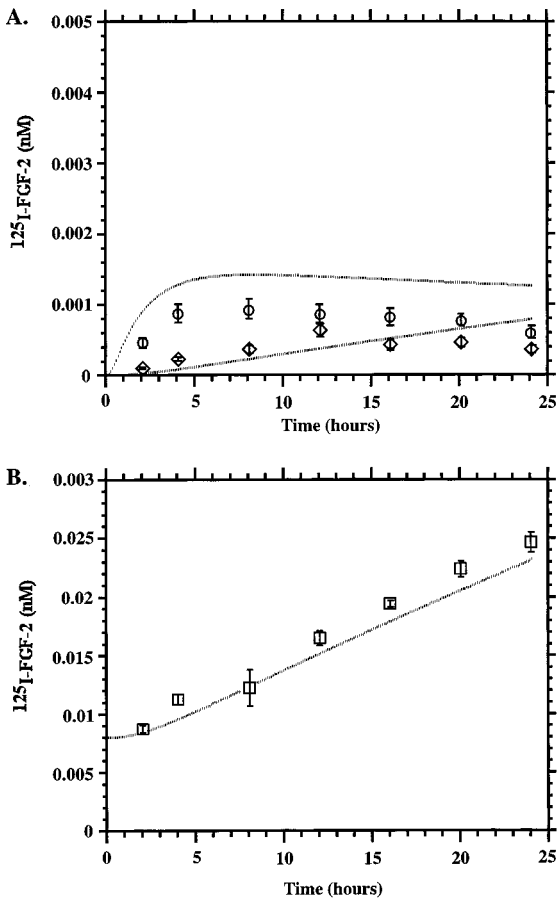

FIGURE 5: FGF-2 processing and secretion within HSPG-deficient VSMC. ^{125}I-FGF-2 was added to native VSMC (0.28 nM) for the indicated times at 37 °C. At each time point, cell-surface-bound FGF-2 was removed, and cells were solubilized in boiling Laemmli sample buffer and applied to an SDS−polyacrylamide gel. Radioactivity in each lane was quantitated by using the phosphorimager. ^{125}I radioactivity was calculated in bands corresponding to 18 + 16 kDa (○) and LMW (◇) (A), and TCA-soluble (degraded FGF-2) radioactivity was measured in the medium (B). The results are the average of triplicate determinations. First-order differential equations (eqs 1−8) were fit to the data to generate the theoretical isotherms (line shown).

slower removal of LMW observed during the pulse chase experiments, indicating that the major pathway of FGF-2 degradation does not include the LMW fragments. Taken together, these data suggest that a primary contributor of FGF-2 accumulation within native cells was the increased production and slow degradation of LMW fragments of FGF-2.

LMW Fragment Formation Is Required for FGF-2 Cytoplasmic Retention. Native VSMC accumulated higher intracellular concentrations of FGF-2 as compared with HSPG-deficient cells (*11*; Figures 1−5). The differences in intracellular levels of FGF-2 could be accounted for by the increased amounts of LMW fragments in native VSMC. If the formation of LMW fragments of FGF-2 was responsible for increased accumulation and high retention of FGF-2 in VSMC, then inhibiting intracellular degradation of FGF-2 might result in a specific reduction in the accumulation of FGF-2 within native VSMC. To test this hypothesis, both native and HSPG-deficient VSMC were treated with the lysosomal inhibitor chloroquine (50 μM) 30 min prior to ^{125}I-FGF-2 addition at 37 °C. At each time point, cell surface FGF-2 was removed for quantitation and the cells were fractionated into cytoplasmic (Figure 6) and nuclear (Figure 7) pools. The cytoplasmic accumulation of FGF-2 was reduced in native cells treated with chloroquine. Chloroquine treatment reduced cytoplasmic accumulation of FGF-2 to levels found in HSPG-deficient cells. Chloroquine addition did not have a significant impact on FGF-2 accumulation in HSPG-deficient cells, consistent with the finding that LMW products do not constitute a high percentage of FGF-2 in these cells. The nuclear accumulation of FGF-2 in native

Table 2: Kinetic Constants for FGF-2 Processing in Native and HSPG-Deficient VSMC[a]

kinetic constants	native VSMC	HSPG-deficient VSMC
k_{LMW} (h^{-1})	0.17	0.026
k_{deg} (h^{-1})	0.45	0.50

[a] The results of the FGF-2 processing studies (Figures 4 and 5), along with values for the amounts of FGF-2 bound to receptors and HSPG on the cell surface, and the endocytosis rate constants (Table 1) were simultaneously fit to eqs 1−8. The computer simulation minimized the difference between the model and the data.

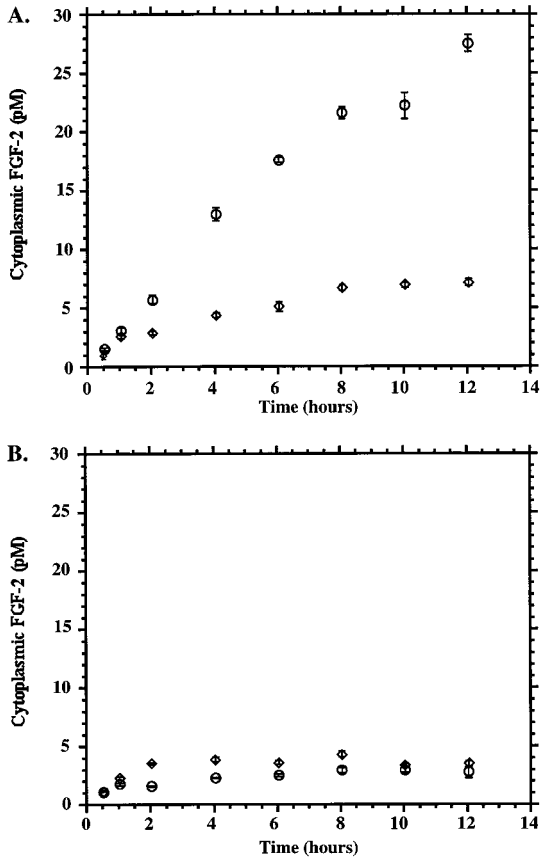

FIGURE 6: Effect of chloroquine on ^{125}I-FGF-2 cytoplasmic uptake in native and HSPG-deficient VSMC. Native (A) and HSPG-deficient (B) VSMC were treated with (◇) or without (○) 50 μM chloroquine for 30 min. ^{125}I-FGF-2 was added at a final concentration of 0.28 nM, and cells were incubated at 37 °C for the indicated times. At each time point, cell-surface-bound FGF-2 was removed, and cells were extracted and fractionated into cytoplasmic and nuclear pools. Radioactivity was quantitated by a γ counter. The results presented represent the averages ± SE of triplicate determinations.

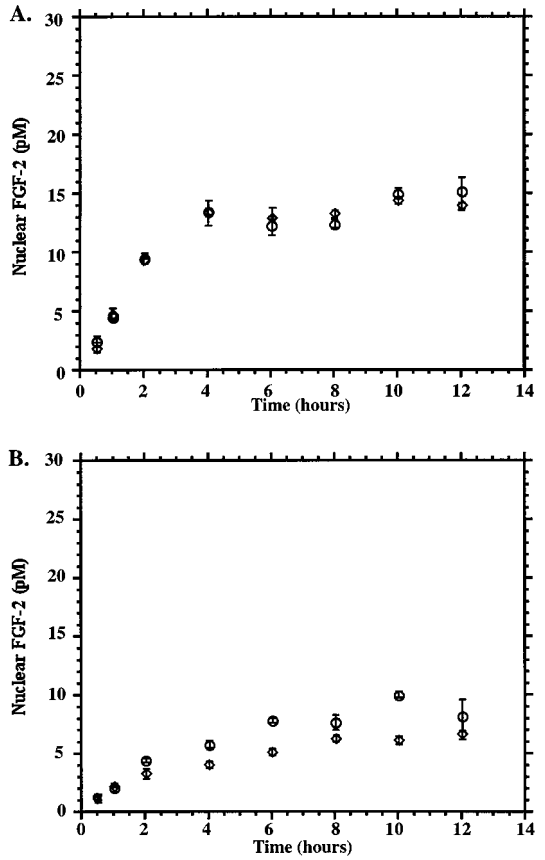

FIGURE 7: Effect of chloroquine on ^{125}I-FGF-2 nuclear uptake in native and HSPG-deficient VSMC. Native (A) and HSPG-deficient (B) VSMC were treated with (◇) or without (○) 50 μM chloroquine for 30 min. ^{125}I-FGF-2 was added at a final concentration of 0.28 nM, and cells were incubated at 37 °C for the indicated times. At each time point, cell-surface-bound FGF-2 was removed, and cells were extracted and fractionated into cytoplasmic and nuclear pools. Radioactivity was quantitated by a γ counter. The results presented represent the averages ± SE of triplicate determinations.

and HSPG-deficient VSMC was virtually unaffected by chloroquine treatment. Taken together, these data suggest that FGF-2 processing was mediated by lysosomes to a large extent. The fact that chloroquine reduced FGF-2 levels specifically in native cells indicated that the processing of FGF-2 was necessary for cellular retention of this growth factor. Nuclear targeting of FGF-2, in contrast, appears to be independent of lysosomal degradation. This is consistent with our previous data as well as that of others, suggesting that mainly intact 18 kDa FGF-2 enters the nuclear compartment (*11*).

Treatment with chloroquine had no effects on cell number or FGF-2 binding to the cell surface in either native or HSPG-deficient VSMC, during the time course of these experiments (data not shown). SDS−PAGE electrophoresis confirmed that cellular degradation of FGF-2 was inhibited. Only 18 kDa FGF-2 was visualized with chloroquine treatment. Treatment with ammonium chloride or leupeptin, additional lysosomal inhibitors, showed similar effects on the intracellular levels of FGF-2. Treatment with the proteosome inhibitor lactacystin (50 μg/mL) did not influence FGF-2 accumulation in either native or HSPG-deficient VSMC (data not shown).

DISCUSSION

HSPG modulation of FGF-2 stability in the extracellular environment has been extensively characterized (*38, 39*). In the extracellular matrix and basement membranes of tissues, HSPG regulate both the bioavailability and the half-life of growth factors by direct physical interaction (*39*). Heparan sulfate and heparin bind and inhibit FGF-2 proteolysis. It has been difficult to establish an intracellular role for HSPG in modulating FGF-2 activity. This has largely been due to the fact that HSPG increase the affinity of FGF-2 for its cell surface receptors and thereby influence the binding and internalization of FGF-2 over the entire course of uptake. Dissecting the role of HSPG in specific steps governing growth factor function distinct from that governed by cell surface receptors has been limited. HSPG have been shown to be constitutively internalized and degraded, by both lysosomal-mediated and nonlysosomal pathways, in rat ovarian granulosa cells *(24, 40)*. These previous studies suggest that the constitutive internalization of HSPG may influence growth factor internalization.

FGF-2 undergoes internalization and degradation once it has gained access to the intracellular environment *(1, 11, 14, 15*). The role of HSPG in the regulation of intracellular processing of FGF-2 has not been extensively studied. In

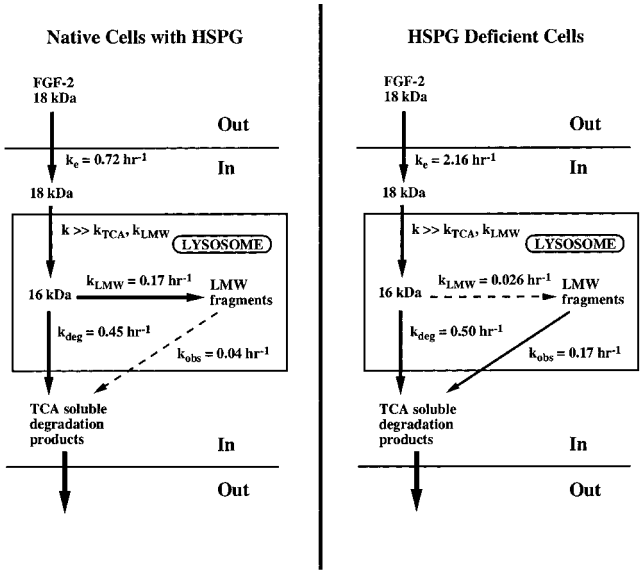

FIGURE 8: Kinetic model of FGF-2 processing in native versus HSPG-deficient VSMC. The various kinetic constants determined from the analyses described in Figures 1−6 and Tables 1 and 2 were incorporated into a simplified model of FGF-2 processing. Native cells containing HSPG (A) are characterized by increased generation and decreased decay of LMW fragments of FGF-2, suggesting that these species are separate from the bulk of FGF-2 that is degraded and excreted as TCA-soluble material. HSPG-deficient cells (B) are characterized by slow formation and rapid decay of LMW fragments such that these species do not appear to be separate from the bulk processing of FGF-2 to small degradation products. Thus the model is consistent with a process where HSPG cause the selective buildup of intracellular pools of LMW fragments of FGF-2. k_{obs} represents the observed first-order rate constant derived from the pulse chase analysis of LMW fragment clearance (Figure 3).

the present study, the role of HSPG in modulating the intracellular half-life of FGF-2 was investigated. The consequences of the presence and absence of HSPG in FGF-2 processing within VSMC was analyzed. Native and HSPG-deficient VSMC were exposed to FGF-2 for various times, to allow for uptake and processing of growth factor. Native VSMC incorporated higher levels of FGF-2 (Figure 2). The increase in FGF-2 incorporation was largely due to the high accumulation of LMW forms of processed FGF-2, which accumulated to high levels within native and not HSPG-deficient VSMC (Figures 1 and 2). LMW fragments of FGF-2 have been shown to be generated in other cell types (*14*, *15*). Both native and HSPG-deficient VSMC were capable of processing FGF-2. However, LMW fragments were stabilized in native VSMC but not in HSPG-deficient cells. It is possible that HSPG either directly interact with LMW fragments of FGF-2 or direct these fragments to intracellular compartments where they are protected from further processing.

The increased accumulation of LMW fragments of FGF-2 within native VSMC is likely the result of increased production and decreased degradation of these fragments (Figure 8). The pulse chase experiments demonstrated that degradation of FGF-2 from 18 to 16 kDa occurred relatively rapidly (with respect to other processes) in both native and HSPG-deficient VSMC and proceeded until LMW intermediates of FGF-2 were formed (Figures 1 and 5). This was consistent with previous results with venular endothelial cells (*14*). However, the further removal of LMW fragments was significantly slowed in native compared to HSPG-deficient cells. Thus, it is possible that an intracellular complex of FGF-2 and heparan sulfate inhibits further processing of FGF-2 within native cells. It may also be that excretion reactions are operating under different regimes in native versus HSPG-deficient VSMC. In native VSMC, where LMW fragment levels are high, the excretion reaction may be limited by other components. In HSPG-deficient VSMC, where LMW fragment levels are low, the excretion reaction may be directly dependent on LMW fragment concentrations.

The rate constants derived by modeling the uptake and processing of FGF-2 as a set of first-order differential equations suggest that the greatest difference between native and HSPG-deficient VSMC was in the formation of LMW fragments, as reflected by the values of k_{LMW} (Table 2). The model results further suggest that the rapid generation of TCA-soluble excreted fragments of FGF-2 in both native and HSPG-deficient cells, as characterized by the relatively large values of k_{deg}, is distinct from the degradation of the LMW fragments. That is, under both conditions the rate constants for degradation product generation were similar and much larger than the apparent rate constants describing the loss of LMW fragments (Table 2, Figure 8). Thus, the LMW fragments appear to represent a selectively stable subpool of internal FGF-2 that is preferred in the presence of HSPG. Since the intracellular levels of the 18 and 16 kDa FGF-2 were similar in both native and HSPG-deficient VSMC, it is unlikely that the increased kinetics of LMW FGF-2 fragment formation in native cells resulted from increased reactant (18 and 16 kDa FGF-2) concentration driving LMW formation. Instead it appears that FGF-2 uptake by lysosomes was occurring at levels nearing saturation for both native and HSPG-deficient VSMC and was not limiting. These data strongly suggest that HSPG specifically modulate intracellular events governing FGF-2 processing. HSPG might act to direct FGF-2 or LMW fragments to other intracellular compartments where rapid degradation is slowed.

To assess whether the increased retention of FGF-2 in native compared to HSPG-deficient cells required lysosomal cleavage, the effect of the lysosomal inhibitor chloroquine (50 μM) was evaluated. The addition of chloroquine to the medium of VSMC reduced the levels of FGF-2 incorporation in native cells to those found in HSPG-deficient VSMC (Figure 7). Whereas chloroquine reduced FGF-2 incorporation in native VSMC, it had virtually no effect on HSPG-deficient cells. These data suggest that a proteolytic event was required for the high retention of FGF-2 in native VSMC. The appearance of FGF-2 in the nuclear fraction was unaffected by chloroquine treatment in both native and HSPG-deficient VSMC. This was consistent with existing literature as well as data from our laboratory confirming that high molecular weight 18 kDa FGF-2 is shuttled to this compartment (*11*).

The retention of FGF-2 for such prolonged periods of time may serve a biological function. It still remains to be determined whether FGF-2 interacts with other intracellular factors to regulate cellular activity. The data presented here strongly suggest that FGF-2 interacts with heparan sulfate once internalized. It may be that the degradation of components involved in a complex of FGF-2/FGFR/HSPG is a requisite for retention of LMW fragments of FGF-2. For example, the processing of either receptor or HSPG may also

be required. Furthermore, the processing of either of these moieties may provide distinct biological functions independent of FGF-2.

The biological function of cell surface receptors and the ligands that interact with them may not be limited to the signaling generated at the cell surface. Internalized cell surface receptors and ligands might have important biological functions. As cells have evolved into very efficient processors of signals, the question arises as to why some growth factors are retained for such prolonged periods after their cell surface role has been fulfilled. Considering that both epidermal growth factor (EGF) and FGF-2 have been shown to activate the MAPK signaling cascade (*41*), it may be that differences in biological action between these mitogens arise from the intracellular processing they undergo. In particular, the persistence of growth factor-mediated signals might ultimately dictate biological response. Indeed, the effects of EGF and nerve growth factor (NGF) on the proliferation and differentiation of PC12 cells represents a classic example of the role for signal persistence (*42*). Whereas both EGF and NGF induce a rapid activation of the MAPK pathway, NGF treatment induces a prolonged activation and differentiation while EGF induces proliferation. Hence, the role of HSPG may be to act as a cellular switch between immediate and prolonged signal activation by heparin-binding growth factors such as FGF-2. In the absence of HSPG, FGF-2 can interact with and activate its receptor (*8*, *43*), yet in the presence of HSPG, FGF-2 might be able to mediate prolonged biological responses through intracellular processes. While the role of internal FGF-2 or fragments of FGF-2 has yet be to demonstrated, it is intriguing to speculate that internalized FGF-2 has novel activities. Furthermore, the large amount of chemical diversity within heparan sulfate as well as the many HSPG core proteins could provide an extremely sensitive system for cells to use to generate unique responses to ubiquitous growth factors.

ACKNOWLEDGMENT

The work was presented as part of a Ph.D. dissertation (G.V.S.) to the Department of Biochemistry. Thus, we thank the Ph.D. dissertation advisory committee and other members of the department for helpful suggestions and valuable discussions.

REFERENCES

1. Bikfalvi, A., Klein, S., Pintucci, G., and Rifkin, D. B. (1997) *Endocr. Rev. 18*, 26−45.
2. Jaye, M., Schlessinger, J., and Dionne, C. A. (1992) *Biochim. Biophys. Acta 1135*, 185−199.
3. Johnson, D. E., and Williams, L. T. (1993) *Adv. Cancer Res. 60*, 1−41.
4. Turnbull, J. E., and Gallagher, J. T. (1993) *Biochem. Soc. Trans. 21*, 477−482.
5. Yayon, A., Klagsbrun, M., Esko, J. D., Leder, P., and Ornitz, D. M. (1991) *Cell 64*, 841−848.
6. Nugent, M. A., and Edelman, E. R. (1992) *Biochemistry 31*, 8876−8883.
7. Nugent, M. A., and Iozzo, R. V. (2000) *Int. J. Cell Biol. Biochem.* (in press).
8. Fannon, M., and Nugent, M. A. (1996) *J. Biol. Chem. 271*, 17949−17956.
9. Rapraeger, A., Krufka, A., and Olwin, B. (1991) *Science 252*, 1705−1708.
10. Horowitz, A., and Simons, M. (1998) *J. Biol. Chem. 273*, 10914−10918.
11. Sperinde, G. V., and Nugent, M. A. (1998) *Biochemistry 37*, 13153−13164.
12. Brown, M. S., Anderson, G. W., and Goldstein, J. L. (1983) *Cell 32*, 663−667.
13. Mellman, I., Fuchs, R., and Helenius, A. (1986) *Annu. Rev. Biochem. 55*, 663−700.
14. Hawker, J. R., and Granger, H. J. (1992) *Am. J. Physiol. 262*, H1525−37.
15. Moenner, M., Gannoun-Zaki, L., Badet, J., and Barritault, D. (1989) *Growth Factors 1*, 115−123.
16. Amalric, F., Baldwin, V., Bosc-Bierne, I., Bugler, B., Couderc, B., Guyader, M., Patry, V., Prats, H., Roman, A. M., and Bouche, G. (1991) *Ann. N.Y. Acad. Sci. 638*, 127−138.
17. Prudovsky, I., Savion, N., Zhan, X., Friesel, R., Xu, J., Hou, J., McKeehan, W. L., and Maciag, T. (1994) *J. Biol. Chem. 269*, 31720−31724.
18. Sadatoshi, B., Shrivastav, S., Yu, Z., Lappi, D. A., Baird, A., and Casscells, W. (1996) *Drug Delivery 3*, 155−163.
19. Reiland, J., and Rapraeger, A. C. (1993) *J. Cell Sci. 105*, 1085−1093.
20. Maher, P. A. (1996) *J. Cell Biol. 134*, 529−536.
21. Amalric, F., Bouche, G., Bonnet, H., Brethenou, P., Roman, A. M., Truchet, I., and Quarto, N. (1994) *Biochem. Pharmacol. 47*, 111−115.
22. Prudovsky, I. A., Savion, N., LaVallee, T. M., and Maciag, T. (1996) *J. Biol. Chem. 271*, 14198−14205.
23. Stachowiak, M. K., Maher, P. A., Joy, A., Mordechai, E., and Stachowiak, E. K. (1996) *Mol. Brain Res. 38*, 161−165.
24. Yanagishita, M., and Hascall, V. C. (1992) *J. Biol. Chem. 267*, 9451−9454.
25. Ishihara, M., Fedarko, N. S., and Conrad, E. H. (1986) *J. Biol. Chem. 261*, 13575−13580.
26. Fedarko, N. S., and Conrad, H. E. (1986) *J. Cell Biol. 102*, 587−599.
27. Castellot, J. J., Cochran, D. L., and Karnovsky, M. J. (1985) *J. Cell. Physiol. 124*, 21−28.
28. Reidy, M. A. (1988) *Lab. Invest. 59*, 36−43.
29. Fritze, L., Reilly, C., and Rosenberg, R. (1985) *J. Cell. Biol. 100*, 1041−1049.
30. Lindner, V., Lappi, D. A., Baird, A., Majack, R. A., and Reidy, M. A. (1991) *Circ. Res. 68*, 106−113.
31. Lindner, V., and Reidy, M. A. (1991) *Proc. Natl. Acad. Sci. U.S.A. 88*, 3739−3743.
32. Edelman, E. R., Nugent, M. A., Smith, L. T., and Karnovsky, M. J. (1992) *J. Clin. Invest. 89*, 465−473.
33. Ross, R. (1971) *J. Cell Biol. 50*, 172−186.
34. Connolly, D. T., Knight, M. B., Harakas, N. K., Wittwer, A. J., and Feder, J. (1986) *Anal. Biochem. 152*, 136−140.
35. Press, W. H., Flannery, B. P., Teukolsky, S. A., and Vetterling, W. T. (1986) *Numerical Recipes*, Cambridge University Press, Cambridge, England.
36. Walicke, P. A., and Baird, A. (1991) *J. Neurosci. 11*, 2249−2258.
37. French, A. R., and Lauffenburger, D. A. (1997) *Ann. Biomed. Eng. 25*, 690−707.
38. Saksela, O., Moscatelli, D., Sommer, A., and Rifkin, D. B. (1988) *J. Cell Biol. 107*, 743−751.
39. Flaumenhaft, R., and Rifkin, D. (1992) *Mol. Biol. Cell 3*, 1057−1065.
40. Yanagishita, M., and Hascall, V. C. (1984) *J. Biol. Chem. 259*, 10270−10283.
41. Scheffer, H. J., and Weber, M. J. (1999) *Mol. Cell. Biol. 19*, 2435−2444.
42. Marshall, C. J. (1995) *Cell 80*, 179−185.
43. Roghani, M., Mansukhani, A., Dell'Era, P., Bellosta, P., Basilico, C., Rifkin, D. B., and Moscatelli, D. (1994) *J. Biol. Chem. 269*, 3976−3984.

BI992243D